Inhibition of neogenin fosters resolution of inflammation and tissue regeneration

Martin Schlegel,[1] Andreas Körner,[1] Torsten Kaussen,[2] Urs Knausberg,[1] Carmen Gerber,[1] Georg Hansmann,[2] Hulda Soffia Jónasdóttir,[3] Martin Giera,[3] and Valbona Mirakaj[1]

[1]Department of Anesthesiology and Intensive Care Medicine, Molecular Intensive Care Medicine, University Hospital Tübingen, Eberhard-Karls University Tübingen, Tübingen, Germany. [2]Department of Pediatric Cardiology and Critical Care, Pulmonary Vascular Research Center, Hannover Medical School, Hannover, Germany. [3]Center for Proteomics and Metabolomics, Leiden University Medical Center (LUMC), Leiden, Netherlands.

The resolution of inflammation is an active process that is coordinated by endogenous mediators. Previous studies have demonstrated the immunomodulatory properties of the axonal guidance proteins in the initial phase of acute inflammation. We hypothesized that the neuronal guidance protein neogenin (Neo1) modulates mechanisms of inflammation resolution. In murine peritonitis, Neo1 deficiency (Neo1$^{-/-}$) resulted in higher efficacies in reducing neutrophil migration into injury sites, increasing neutrophil apoptosis, actuating PMN phagocytosis, and increasing the endogenous biosynthesis of specialized proresolving mediators, such as lipoxin A4, maresin-1, and protectin DX. Neo1 expression was limited to Neo1-expressing Ly6C^{hi} monocytes, and Neo1 deficiency induced monocyte polarization toward an antiinflammatory and proresolving phenotype. Signaling network analysis revealed that Neo1$^{-/-}$ monocytes mediate their immunomodulatory effects specifically by activating the PI3K/AKT pathway and suppressing the TGF-β pathway. In a cohort of 59 critically ill, intensive care unit (ICU) pediatric patients, we found a strong correlation between Neo1 blood plasma levels and abdominal compartment syndrome, Pediatric Risk of Mortality III (PRISM-III) score, and ICU length of stay and mortality. Together, these findings identify a crucial role for Neo1 in regulating tissue regeneration and resolution of inflammation, and determined Neo1 to be a predictor of morbidity and mortality in critically ill children affected by clinical inflammation.

Introduction

There are only a few targeting therapies for critically ill patients in the intensive care unit (ICU) who are suffering from complex and potentially life-threatening illnesses, such as acute respiratory distress syndrome and multiple organ failure. Hence, severe inflammation is recognized as a considerable problem in the care of these critically ill patients when resolution of inflammation fails to induce homeostasis (1). It is evident that nonresolving inflammation may lead to the activation of chronic inflammatory processes and ultimately to the development of organ dysfunction and the incurrence of comorbidities (2, 3). The initiation of this pivotal process is guided by diverse classes of mediators including cytokines, chemokines, and lipid mediators (3, 4). These mediators initiate the influx of proinflammatory cells that cause tissue injury. Following the initiation of an inflammatory response, when self-limited, a superfamily of endogenous mediators (SPMs) is generated to activate processes for resolution, indicating that the resolution of inflammation is a process that is distinct from antiinflammatory mechanisms (5). The key steps in this phase include (a) cessation of further PMN influx, (b) normalization of chemokine/cytokine gradients, (c) apoptosis of PMNs, (d) activation of macrophage (MΦ) phagocytosis and efferocytosis, and (e) generation of endogenous proresolving mediators (i.e., SPMs).

A paradigm for neuronal guidance proteins (NGPs) and their target receptors exists in the developing nervous system, where neuronal movement is mediated by the interplay of both attractive and repulsive signals. Analogies with axonal migration have postulated that these NGPs play an important role outside the central nervous system in guiding leukocyte migration (6–11). Neo1, a type I transmembrane protein and receptor for Netrin-1 and the repulsive guidance molecules (RGMs), is recognized to be essential in neurogenic and embryonic processes, in which it contributes to chondrogenesis, myogenesis, organ-specific development of the mammary gland, and neural tube formation (12–14). Recent studies have shown Neo1 to have pivotal nonneuronal functions during the onset of acute inflammation (9, 15, 16). However, the primary issue with inflammation is not the frequency of its initiation, but rather the formation of excessive or unresolved processes (2, 5). This notion, coupled with its immunomodulatory attributes, led us to question whether Neo1 might contribute to local inflammation resolution mechanisms and tissue regeneration processes.

Our studies revealed that functional inhibition of Neo1 induced apoptosis of neutrophils, which is a key feature of the initiation of the inflammation resolution mechanism (17) and ultimately shortened the neutrophil lifespan. Functional inhibition of Neo1 activated eat-me and find-me signals and G pro-

Authorship note: MS and AK contributed equally to this work.
Conflict of interest: The authors have declared that no conflict of interest exists.
Submitted: July 14, 2017; **Accepted:** July 26, 2018.
Reference information: *J Clin Invest*. 2018;128(10):4711–4726.
https://doi.org/10.1172/JCI96259.

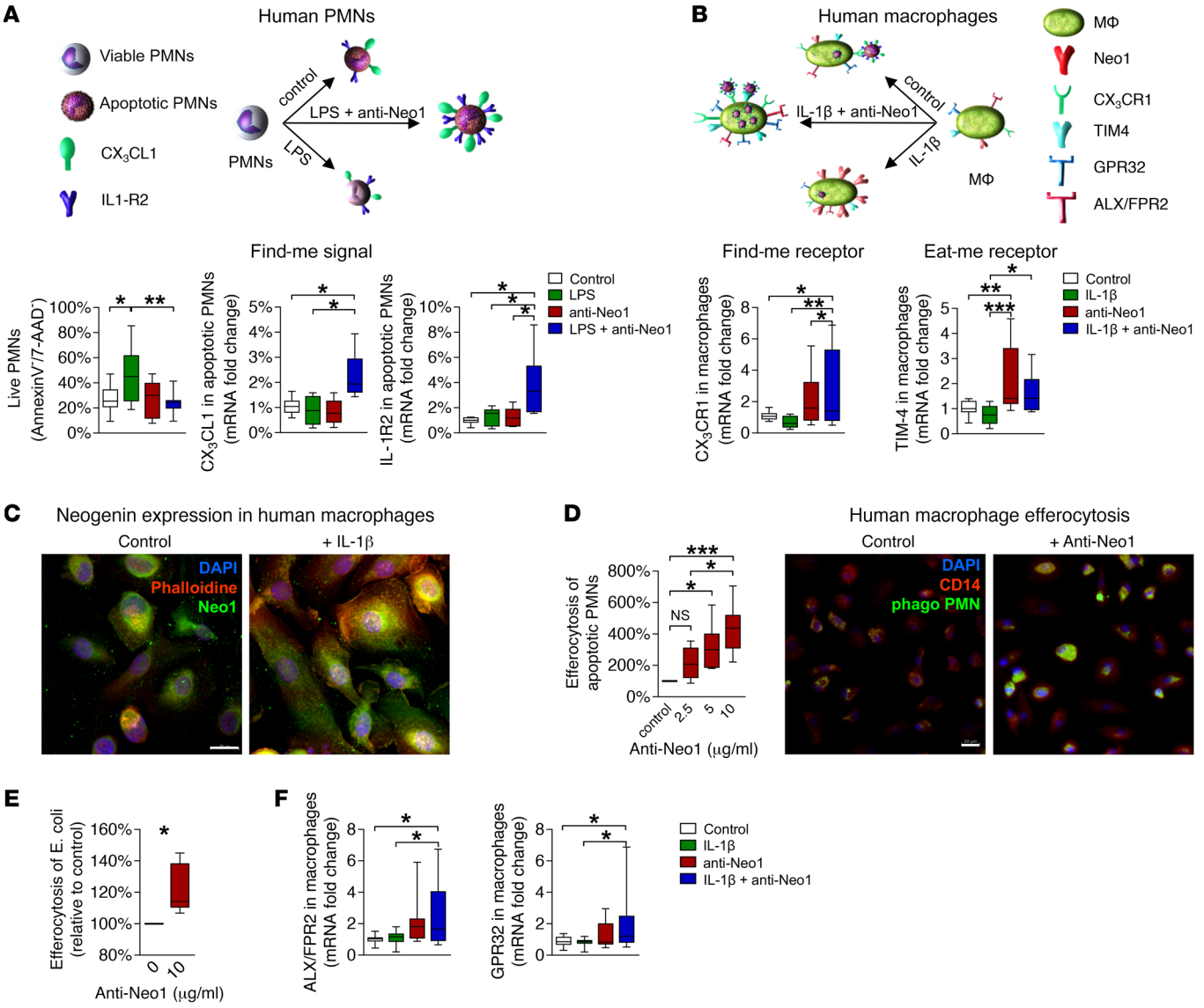

Figure 1. Role of Neo1 on human PMN apoptosis and MΦ efferocytosis. (**A**) Apoptosis of human PMNs following LPS and/or anti-Neo1 stimulation was determined by flow cytometry and the expression of CX_3CL1 mRNA and IL-1R2 mRNA was evaluated by RT-PCR. (**B**) Human MΦ were stimulated with IL-1β and/or anti-Neo1 antibody and the CX_3CR1 mRNA and TIM4 mRNA levels were determined by RT-PCR. (**C**) Neo1 protein expression was assessed by immunofluorescence staining (n = 3/condition, magnification ×630, scale bar 20 μm). (**D**) The dose-dependent impact of anti-Neo1 treatment on MΦ clearance of the apoptotic PMNs and the corresponding immunofluorescence images (n = 3/condition, magnification ×400, scale bar 20 μm). (**E**) MΦ efferocytosis of *E. coli*. (**F**) mRNA expression of the ALX/FPR2 and GPR32 receptors in human MΦ. Results represent 2 independent experiments and are expressed as median ± 95% CI (n = 6–8 per group). Statistical analysis was done by ANOVA followed by Bonferroni's post hoc test, $^*P < 0.05$, $^{**}P < 0.01$, $^{***}P < 0.001$.

tein–coupled receptors (GPCRs) in human apoptotic PMNs or macrophages (MΦ) to mediate proresolving actions. In a model of murine peritonitis, we found that deficiency of Neo1 led to antiinflammatory, proresolving, and proregenerative effects, as shown by reduced PMN infiltration to the site of inflammation, increased neutrophil apoptosis, enhanced local clearance via phagocytosis of apoptotic cells, and the biosynthesis of local endogenous proresolving lipid mediators (i.e., lipoxin A4 [LXA_4], maresin-1 [Mar1], and protectin DX [PDX]). Neo1 expression was particularly restricted to the inflammatory peritoneal Ly6C^{hi} cells, and Neo1 deficiency induced monocyte polarization toward the proresolving and prohealing Ly6C^{lo} phenotype. Bone marrow transplant chimeric mouse experiments showed hematopoietic Neo1 repression to be crucial for the reduction of Ly6C^{hi} monocytes, the increase of Ly6C^{lo} monocytes, and finally, the increase in clearance. In our analysis, we found Neo1$^{-/-}$ monocytes to activate the PI3K/AKT pathway and suppress the TGF-β pathway, both of which are critical in restricting proinflammatory and promoting antiinflammatory responses and activating the monocyte and monocyte-derived MΦ polarization toward the proresolving phenotype. In line with these results, in an observational clinical study that included 59 critically ill ICU pediatric patients suffering from, in part, intraabdominal hypertension (IAH), abdominal compartment syndrome (ACS), internal cardiac and oncolog-

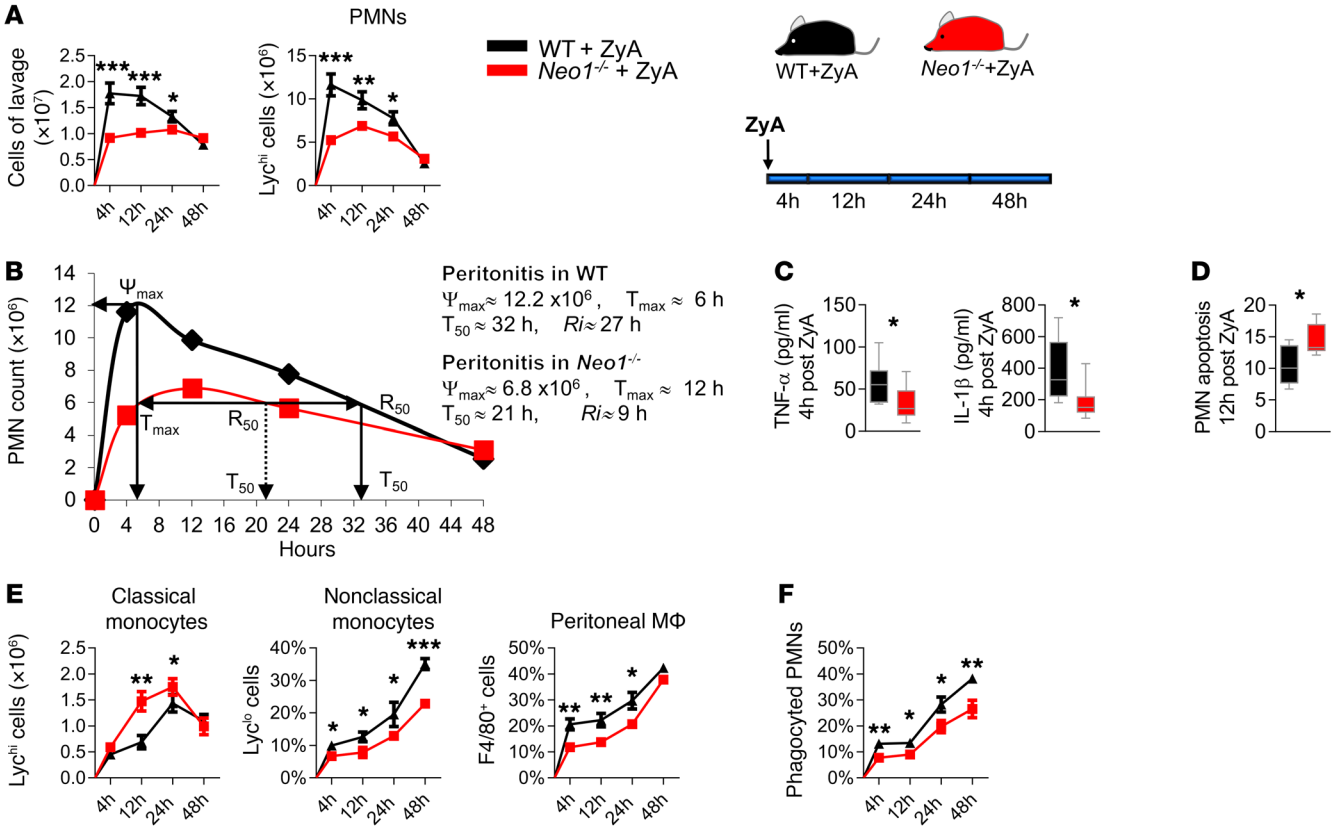

Figure 2. Targeted deletion of Neo1 promotes resolution of acute inflammation. *Neo1*$^{-/-}$ mice and their littermate controls were exposed to ZyA-induced peritonitis, and peritoneal lavages were collected at 4, 12, 24, and 48 hours. (**A**) The leukocyte total was enumerated by light microscopy and the PMNs were determined by flow cytometry. (**B**) Resolution indices, as previously defined (41). (**C**) The IL-1β and TNF-α levels were measured in the peritoneal fluids (4 hours after ZyA injection). (**D**) Apoptotic PMNs (12 hours after ZyA injection), (**E**) classical Ly6C^{hi} monocytes, nonclassical Ly6C^{low} monocytes, F4/80^{+} peritoneal MΦ, and (**F**) monocyte-derived MΦ efferocytosis were determined by flow cytometry. The results represent 2 independent experiments and are expressed as mean ± SEM (**A**, **E**–**F**) and as median ± 95% CI (**C**, **D**) (n = 8–12 per group). Statistical analysis was done by unpaired Student's t test, $^{*}P < 0.05$, $^{**}P < 0.01$, $^{***}P < 0.001$.

ical diseases, or being cared for after surgical interventions, we found a strong correlation among plasma Neo1 levels and IAH, ACS, severity of illness, ICU length of stay, and survival.

Our studies indicate a critical role for Neo1 in controlling processes involved in the inflammation resolution and tissue regeneration phases, and they may represent an advance in our understanding of the pathways that can restrain or promote the resolution of inflammation. In turn, our data may help identify new potential targets in diseases of major global health significance.

Results

Impact of Neo1 on human PMN apoptosis and macrophage efferocytosis. It is now evident that the failed clearance of dying cells alters immune tolerance and promotes nonresolving inflammation (2, 17). In the early phase of inflammation, apoptosis of neutrophils induces neutrophil functional shutdown, which is a key feature of the initiation of inflammation resolution mechanisms (18, 19). We therefore sought to investigate whether Neo1 plays a role in the apoptosis of neutrophils. Human PMNs were stimulated with vehicle or LPS (100 ng/ml) and/or anti–Neo1 antibody (Ab) and then allowed to undergo apoptosis for 20 hours. Functional inhibition of Neo1 induced the apoptosis of neutrophils, suggesting that anti-Neo1 treatment shortened the neutrophil lifespan (Figure 1A). In apoptotic PMNs, blockade of Neo1 induced the expression of the decoy receptor IL-1R2, which is known for its strong impact on limiting the proinflammatory effects of IL-1β (Figure 1A) (20). It is evident that apoptotic neutrophils induce their own clearance by expressing find-me and eat-me signals (17, 21). Therefore, we sought to determine the expression of CX_3CL1, a critical protein contributing as a find-me signal in MΦ, and its receptor CX_3CR1, which is crucial for sensing chemokines and recruiting monocytes (22). We found that blockade of Neo1 markedly increased both the CX_3CL1 mRNA in apoptotic PMNs and the CX_3CR1 mRNA in MΦ. These data were substantiated by increased levels of one of the most crucial eat-me receptors, TIM4, which mediates the direct recognition of phosphatidylserine by MΦ. (Figure 1B). In addition to neutrophil apoptosis, MΦ efferocytosis is a key feature of resolution programs. We therefore set out to investigate the expression of Neo1 in human MΦ and PMNs (Figure 1C and Supplemental Figure 1; supplemental material available online with this article; https://doi.org/10.1172/JCI96259DS1). Our data revealed a strong induction of Neo1 expression in MΦ following IL-1β stimulation. We found that the functional inhibition of Neo1 significantly increased the phagocytosis rate in a dose-dependent manner. These results were confirmed by immunofluorescence analysis (Figure 1D). In subsequent *E. coli* efferocytosis studies as a surro-

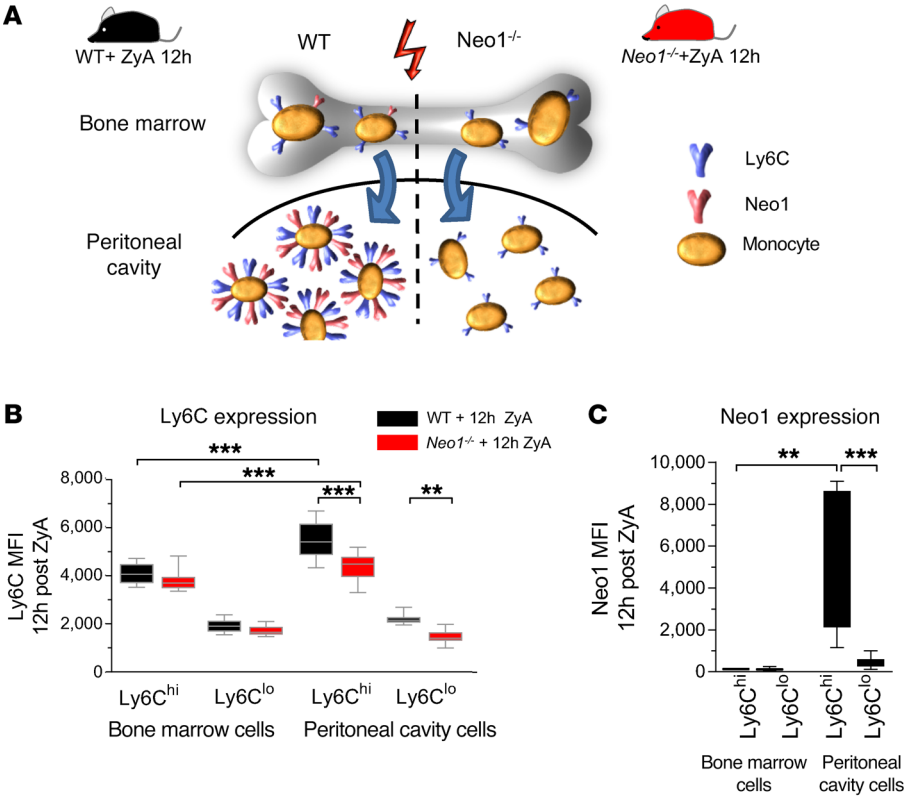

Figure 3. Neo1-dependent monocyte intracellular signaling. WT and *Neo1*$^{-/-}$ bone marrow monocytes and WT and *Neo1*$^{-/-}$ peritoneal monocytes were collected 12 hours after ZyA injection. (**A**) Schematic illustration of maturation patterns in WT and Neo1$^{-/-}$ monocytes. (**B**) Ly6C expression and (**C**) Neo1 expression in bone marrow monocytes and peritoneal monocytes were determined by flow cytometry. The results represent 2 independent experiments and are expressed as median ± 95% CI (n = 8–12 per group). Statistical analysis was done by 1-way ANOVA followed by Bonferroni's post hoc test, *$P < 0.05$, **$P < 0.01$, ***$P < 0.001$.

gate for infection-resolving actions, we were able to corroborate our results (Figure 1E). Given that GPCRs such as ALX/FPR2 and DRV1/GPR32 have been shown to mediate proresolving actions (23), we demonstrated that stimulation with anti-Neo1 plus IL-1β significantly augmented the mRNA levels of these 2 receptors in MΦ (Figure 1F). These findings showed that functional inhibition of Neo1 plays an important regulatory role in resolving inflammation, by sensing and detecting dying and apoptotic neutrophils in the early stages of inflammation and by phagocytizing and subsequently removing them in later stages of inflammation.

Mice deficient in Neo1 display a reduction in PMN recruitment, enhancement of neutrophil apoptosis, and augmentation of efferocytosis. Based on the results described above, we hypothesized that Neo1 is a major player in the active resolution of acute inflammatory responses. As mentioned before, key characteristics of resolution are the cessation of neutrophil migration, the enhancement of uptake and clearance of apoptotic cells and microorganisms in inflamed tissues, and the biosynthesis of proresolving mediators (5). Using mice deficient in Neo1 (Neo1$^{-/-}$), we modeled a self-limited resolving murine peritonitis and examined the cellular events in both the early phase and the resolution phase. In a time series (4 hours, 12 hours, 24 hours, and 48 hours), wild-type (WT) littermates displayed maximal PMN infiltration at 4 hours in the peritoneal exudates (Figure 2A), followed by a reduction, providing a resolution interval (Ri) of 27 hours. In Neo1$^{-/-}$ mice, we found a strong reduction in leukocyte recruitment, with a shift of maximal PMNs to 12 hours and a resolution interval of 9 hours (Figure 2B). Additionally, TNF-α and IL-1β, 2 well-known proinflammatory cytokines that mediate the inflammatory response and contribute to apoptotic cell death, were significantly decreased (Figure 2C). Neutrophil apoptosis, as an important control point in resolution processes, was enhanced in Neo1$^{-/-}$ mice compared with the littermate control animals (Figure 2D). This was accompanied by a significant reduction in the classical Ly6C^{hi} monocytes and an increase in the alternatively activated Ly6C^{lo} monocytes and peritoneal MΦ Neo1$^{-/-}$ mice versus controls (Figure 2E). In this context, the phagocytosis of apoptotic neutrophils was strongly enhanced in Neo1$^{-/-}$ mice, suggesting that Neo1 affects a delayed-resolution phenotype in acute peritonitis (Figure 2F). To underline the influence of Neo1 on the resolution phase, we then measured the levels of IL-6, KC, MIP2, and MCP-1 within the peritonitis lavages collected 12 hours after zymosan A (ZyA) injection and found significantly decreased levels in Neo1-deficient exudates compared with WT controls (Supplemental Figure 2A). To further substantiate the temporal pattern of Neo1-mediated influence on efferocytosis and tissue homeostasis, we collected peritoneal MΦ either from WT or Neo1$^{-/-}$ mice, and the phagocytosis of fluorescent ZyA particles was determined at 2, 4, and 6 hours after injection. Our data demonstrate that depletion of Neo1 markedly increases the phagocytosis rate at the indicated time points (Supplemental Figure 2B). Together, these data point to a role for Neo1 in the initiation and resolution of inflammatory processes, particularly in the removal of apoptotic cells.

Neo1 expression is confined to peritoneal Ly6C^{hi} monocytes. After demonstrating that Neo1 controls apoptosis and phagocytosis programs in vitro and in vivo, we next aimed to investigate more precisely the role of Neo1 in the regulatory mechanisms underlying these processes. It is evident that monocytes derived from precursors in the bone marrow circulate first in the blood, and from there into tissues to mature to macrophages (24). Knowing that Ly6C is mainly expressed on the migrating inflammatory mono-

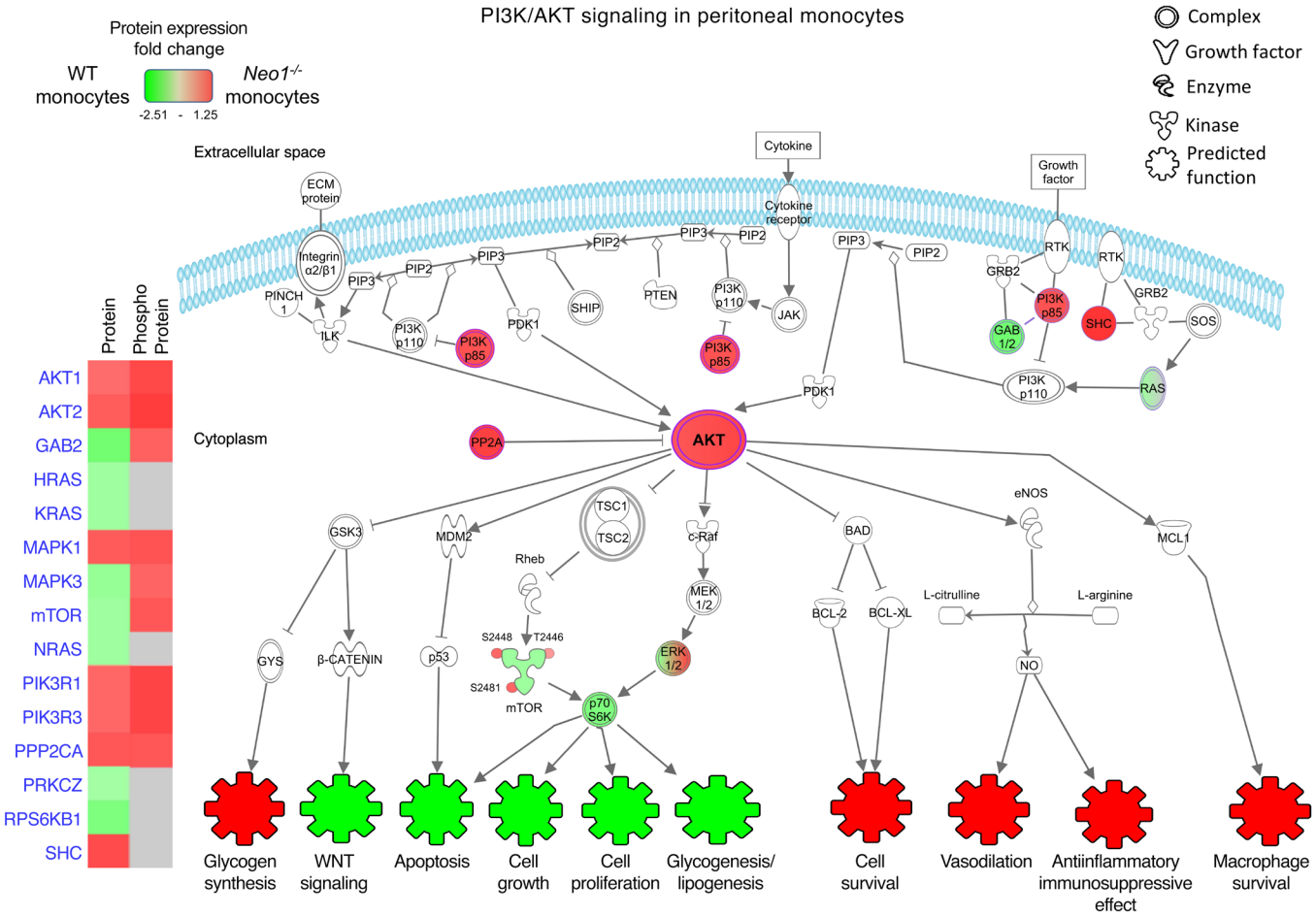

Figure 4. Neo1-dependent monocyte intracellular signaling in the PI3K/AKT pathway. The PI3K/AKT signaling pathway was assessed in peritoneal monocytes by using a protein microarray. Samples were pooled from 4 mice in each group for each experiment.

cyte population with less expression on the alternatively activated monocytes (25), we determined the Ly6C expression in bone marrow monocytes (BMMs) and the peritoneal monocytes in WT and *Neo1*$^{-/-}$ mice 12 hours after ZyA injection. Interestingly, we found that proinflammatory Ly6C^{hi} monocytes had increased Ly6C expression after leaving the bone marrow and migrating into the peritoneal cavity (Figure 3, A and B). This increase in Ly6C expression was significantly reduced in peritoneal *Neo1*$^{-/-}$ monocytes compared with littermate controls. We then examined the Neo1 expression in BMMs and peritoneal monocytes and found Neo1 expression to be specifically restricted to the peritoneal inflammatory Ly6C^{hi} monocytes (Figure 3C).

To more precisely determine the migration patterns of Ly6C^{hi} monocytes, we generated chimeric animals through bone marrow transplantation between Neo1$^{+/+}$ and Neo1$^{-/-}$ mice and vice versa, with WT to Neo1$^{+/+}$ and Neo1$^{-/-}$ to Neo1$^{-/-}$ transplanted animals as controls for nonspecific radiation effects. We then exposed the chimeric animals to ZyA peritonitis and analyzed the cellular events in defined time intervals (4 hours and 12 hours). Bone marrow chimeric animals with hematopoietic Neo1 repression demonstrated a strong reduction in the classical Ly6C^{hi}, an increase in the nonclassical Ly6C^{lo} monocytes, and finally an increase of the MΦ phagocytosis of apoptotic PMNs in both time points (Supplemental Figure 3, A and B). Ly6C, known to be mainly expressed on migrating proinflammatory monocytes, was significantly reduced in peritoneal Neo1$^{-/-}$ monocytes compared with littermate controls (Figure 3B). This effect was also reflected in the bone marrow chimeric animals with hematopoietic Neo repression (Supplemental Figure 3C). We were able to show that Ly6C MFI is strongly decreased in Ly6C^{hi} cells in bone marrow chimeric animals with hematopoietic Neo repression, suggesting that Neo1 impacts the proinflammatory Ly6C^{hi} monocytes. These findings suggest that upon activation and migration to the site of inflammation, Ly6C^{hi} monocytes induce Neo1 expression, enabling them to contribute to the immune response.

Neo1-dependent monocyte intracellular signaling. To investigate the mechanisms by which Neo1 impedes the resolving/regenerative effects, peritoneal monocytes from WT and *Neo1*$^{-/-}$ mice were collected for microarray analysis 12 hours after ZyA induction of peritonitis (Figure 4 and Figure 5). Analysis of protein microarray data demonstrated that Neo1$^{-/-}$ monocytes activate the PI3K/AKT pathway, which is crucial in restricting proinflammatory responses, promoting antiinflammatory responses, and activating the monocyte differentiation and polarization toward a proresolving phenotype (Figure 4, Figure 5B, Supplemental Figure 1, and Supplemental Table 1) (26, 27). The

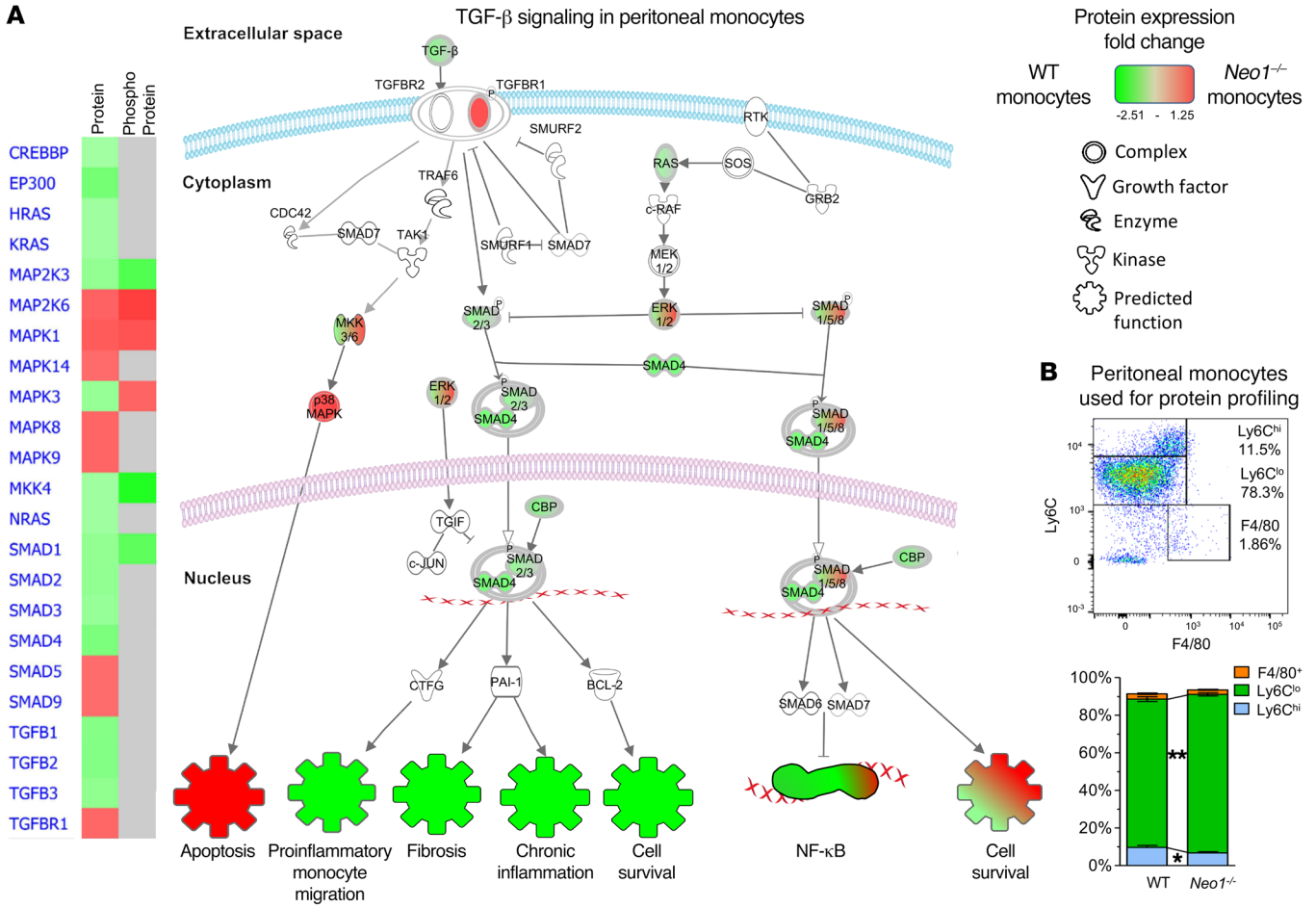

Figure 5. Neo1-dependent monocyte intracellular signaling in the TGF-β pathway. (**A**) The TGF-β signaling pathway was assessed in peritoneal monocytes by using a protein microarray. (**B**) Representative flow cytometry plot and bar chart showing the peritoneal monocytes used for protein profiling. Samples were pooled from 4 mice in each group for each experiment.

expression and/or phosphorylation of enzymes such as AKT1, AKT2, MAPK1, MAPK3, mTOR, PIK3R1, and PIK3R3, which are required for AKT activity, were increased in Neo1$^{-/-}$ monocytes. The TGF-β pathway plays divergent roles in the innate immune system (28). Our microarray data on Neo1$^{-/-}$ monocytes revealed TGF-β signaling to be activated specifically in the context of cell apoptosis, whereas in WT monocytes TGF-β signaling is induced and associated with proinflammatory monocyte migration, fibrosis, chronic inflammation, and cell survival (Figure 5A, Supplemental Figure 4, and Supplemental Table 1). Collectively, these findings provide evidence that deficiency of Neo1 contributes to proresolving and proregenerative actions in monocytes and ultimately in MΦ, and this action is associated with the PI3K/AKT/mTOR and TGF-β signaling pathways.

Impact of Neo1 on lipid mediator biosynthesis. The SPMs — namely, lipoxins, resolvins, protectins, and maresins — have been identified as important determinants of inflammation resolution (5). To examine whether Neo1 impacts the generation of SPMs during inflammation resolution, we carried out liquid chromatography–tandem mass spectrometry–based (LC-MS/MS-based) profiling. In inflammatory peritoneal exudates obtained from Neo1$^{-/-}$ mice and their littermate controls, we identified SPMs as well as their precursors and pathway markers. Specifically, we identified arachidonic acid–derived LXA_4 (Figure 6, A and D), docosahexanoic acid–derived (DHA-derived) PDX (also referred to as 10S,17S-diH-DHA), and Mar1 to be increased in Neo1$^{-/-}$ (Figure 6, B and D). It is well appreciated that prostanoids such as PGD_2, PGE_2, and PGI_2 elicit immunomodulatory and antiinflammatory effects (23, 29–31). In particular, PGD_2 and PGE_2, which are known to induce the inflammatory response, subsequently stimulate antiinflammatory effects by activating the 15-LOX in neutrophils to ultimately promote lipid mediator class-switching during the resolution of acute inflammation. Our data demonstrate the enhanced production of PGD_2 and PGE_2 in the initial phase, suggesting that the mediator class switch is implemented in the resolution phase (Figure 6A and Supplemental Table 2) (31). We also found enhanced levels of the arachidonic acid–derived products 5-hydroxyeicosatetraenoic acid (5-HETE) and 15-HETE, and the eicosapentaenoic acid–derived (EPA-derived) 15-hydroxyeicosapentaenoic acid (15-HEPE) and 18-HEPE in Neo1$^{-/-}$ (Figure 6, A and C). Furthermore, metabolites 14,15-diHETE and 19,20-DiHDPA produced by cytochrome P450 epoxygenases, and the actions of soluble epoxidehydrolase (sEH), thus belonging to a different class of antiinflammatory and proresolving lipids, were also significantly increased in Neo1-deficient mice (Figure 6, A and B). Knowing that the enzymes 5-LOX and 12/15-LOX contribute to the generation of proresolving mediators

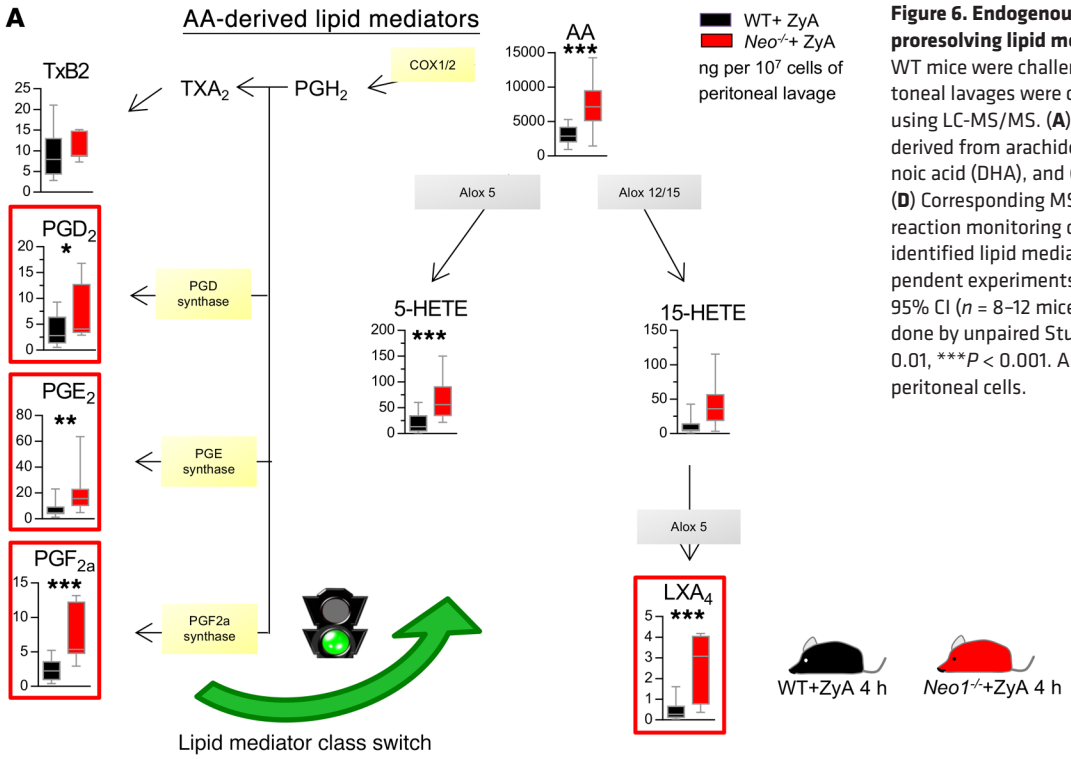

Figure 6. Endogenous deficiency of Neo1 activates proresolving lipid mediator biosynthesis. *Neo1*$^{-/-}$ and WT mice were challenged with ZyA peritonitis. Peritoneal lavages were collected at 4 hours and analyzed using LC-MS/MS. (**A**) Lipid mediators and precursors derived from arachidonic acid (AA), (**B**) docosahexaenoic acid (DHA), and (**C**) eicosapentaenoic acid (EPA). (**D**) Corresponding MS/MS spectra and the multiple reaction monitoring chromatograms (MRM) for the identified lipid mediators. Results represent 3 independent experiments and are expressed as median ± 95% CI (n = 8–12 mice/group). Statistical analysis was done by unpaired Student's t test, $^{*}P < 0.05$, $^{**}P < 0.01$, $^{***}P < 0.001$. All results are reported as ng/10^7 peritoneal cells.

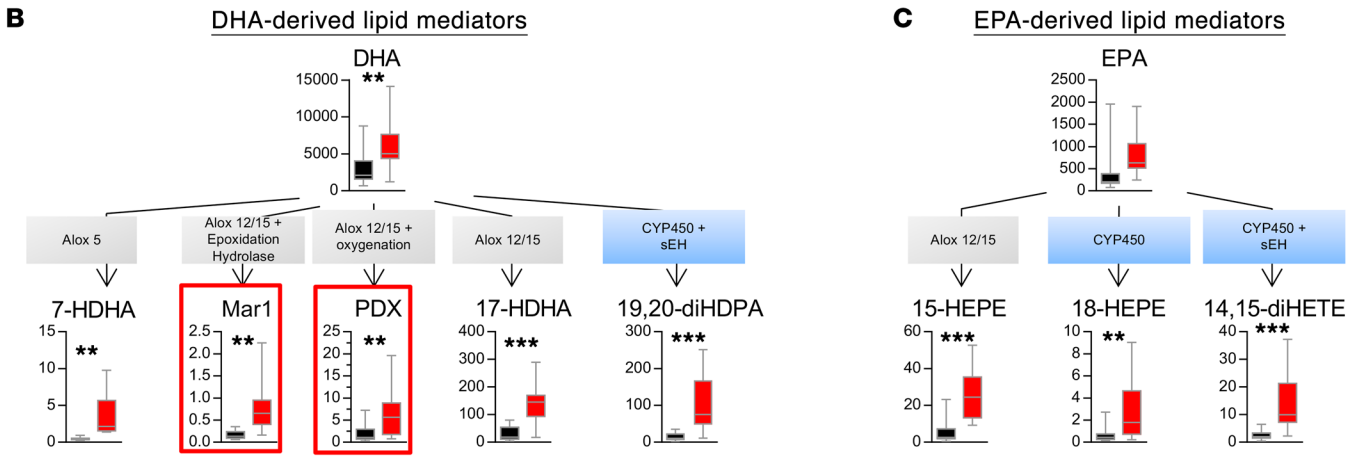

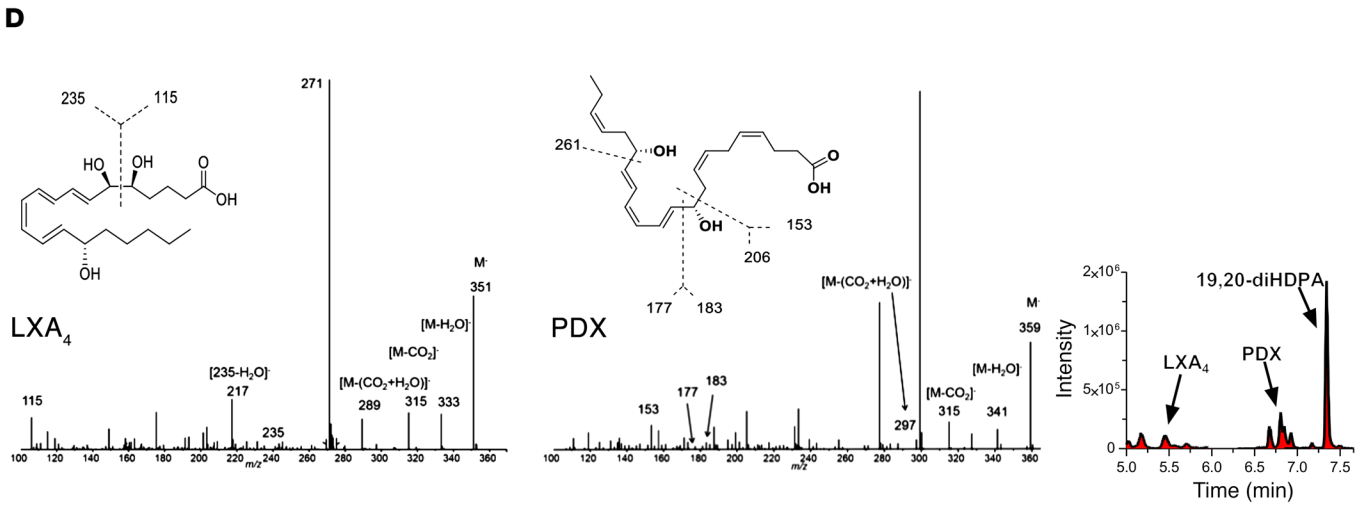

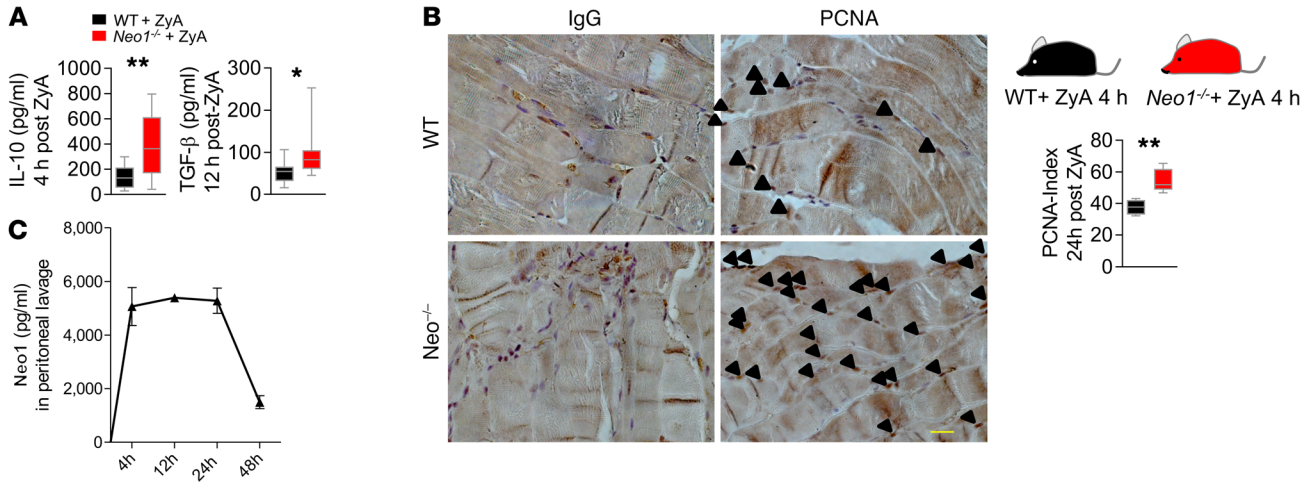

Figure 7. Functional inhibition of Neo1 promotes the resolution and regeneration processes. *Neo1*$^{-/-}$ and WT littermate controls were exposed to ZyA, and peritoneal lavages were collected at 4, 12, 24, and 48 hours. (**A**) Exudate levels of IL-10 (after 4 hours) and TGF-β (after 12 hours). (**B**) Regeneration of the peritoneum was evaluated by PCNA immunohistochemistry staining of the peritoneum (24 hours after ZyA) (n = 4/condition, magnification ×630, scale bar 200 μm) and the calculated index. (**C**) Temporal regulation of Neo1 in ZyA-induced peritonitis exudates measured by ELISA. The results represent 2 independent experiments and are expressed as median ± 95% CI (**A**) and mean ± SEM (**C**) (n = 8–12 per group). Statistical analysis was done by unpaired Student's t test, $^{*}P < 0.05$, $^{**}P < 0.01$.

and finally to increased resolution effects, we incubated peritoneal MΦ from WT or 12/15-LOX–deficient mice with Neo1 Ab and found a reduced efferocytosis rate of fluorescence-labeled ZyA particles after stimulation with Neo1 Ab (Supplemental Figure 6D). In a second set of experiments, we incubated peritoneal MΦ from WT or Neo1$^{-/-}$ mice with 5-LOX and 12/15-LOX inhibitors baicalein or cinnamyl-3,4-dihydroxy-α-cyanocinnamate (CDC) and found a reduced ZyA efferocytosis rate in Neo1$^{-/-}$ cells (Supplemental Figure 6E). To substantiate these data we incubated human MΦ with Neo1 Ab and baicalein or CDC. The impact of Neo1 inhibition on MΦ phagocytosis was significantly reduced when costimulated with 5-LOX and 12/15-LOX inhibitors, suggesting that the Neo1 effects on resolution are 5-LOX and 12/15-LOX dependent (Supplemental Figure 6F). This result is consistent with the increased biosynthesis of the 5-LOX– and 12/15-LOX–dependent proresolving mediators, such as LXA_4, Mar1, and PDX in the Neo1$^{-/-}$ mice.

Taken together, these results strongly highlighted that targeted deletion of Neo1 modulates the lipid mediator profile in murine exudates toward an antiinflammatory and proresolving state.

Genetic deletion of Neo1 contributed to tissue regeneration mechanisms in vivo. After demonstrating that genetic deletion of Neo1 promoted key resolution features, we turned our attention to the influence of Neo1 on tissue repair/regeneration and found increased levels of IL-10 and TGF-β peritonitis exudate, 2 parameters contributing to peritoneal tissue repair and regeneration in Neo1$^{-/-}$ mice (Figure 7A) (2, 18, 32). This is in line with our cellular data that shows Neo1$^{-/-}$ monocytes activate the PI3K/AKT pathway for the induction of cell polarization toward the M2 phenotype. To substantiate this proregenerative impact, we performed a staining for proliferating cell–nuclear antigen (PCNA) within the peritoneum, which displayed an index increase of approximately 20% in Neo1$^{-/-}$ peritonitis compared with the WT group (Figure 7B). Since our data revealed Neo1 to be a negative regulator in the resolving and regenerative processes, we next elucidated the temporal regulation of Neo1 during the initiation and resolution phase (Figure 7C). Exudate Neo1 was markedly increased between 4 hours and 24 hours and subsequently decreased at the end of the resolution phase, suggesting that Neo1 impacts processes during initiation and resolution/regeneration of acute inflammation. To clarify whether Neo1 expression is cell type–specific and not only related to the cell trafficking events, we determined the Neo1 expression on cellular exudates and found Neo1 to be strongly increased between 4 hours and 12 hours, followed by a decrease at the end of the resolution phase (Supplemental Figure 5).

Functional inhibition of Neo1 promotes the resolution and regeneration processes. Having shown that endogenous deletion of Neo1 initiated the resolution of acute inflammation by inducing the apoptosis of PMNs, the cessation of PMN influx, efficient clearance of PMNs, and the biosynthesis of SPMs, we next sought to investigate whether anti-Neo1 has any therapeutic efficacy in acute inflammation (e.g., potentially resolving processes such as peritonitis). When a functional anti-Neo1 Ab was given as a prophylactic treatment (in parallel with ZyA injection) for murine peritonitis, WT mice displayed reduced PMN infiltration and shortened resolution interval, from 26 hours to 7 hours (Figure 8, A and B). Furthermore, administration of an anti-Neo1 Ab decreased classical Ly6C^{hi} monocytes and increased nonclassical Ly6C^{lo} monocytes and MΦ, which led to strong enhancement of MΦ clearance of apoptotic PMNs (Figure 8C). Also, the inflammation-initiated cytokines, such as TNF-α, IL-1β, IL-6, and keratinocyte chemoattractant (KC, IL-8 in humans), were reduced (Figure 8D). In a second set of experiments, we investigated the therapeutic administration of an anti-Neo1 Ab. The agent was given at the peak of inflammation as monitored by maximal neutrophil recruitment, and peritoneal lavages were collected at 12, 24, and 48 hours. As expected, we found activation of cardinal signs of resolution with a shortening of the resolution interval from 23 hours to only 16 hours (Figure 9, A and B), suggesting a stronger treatment effect

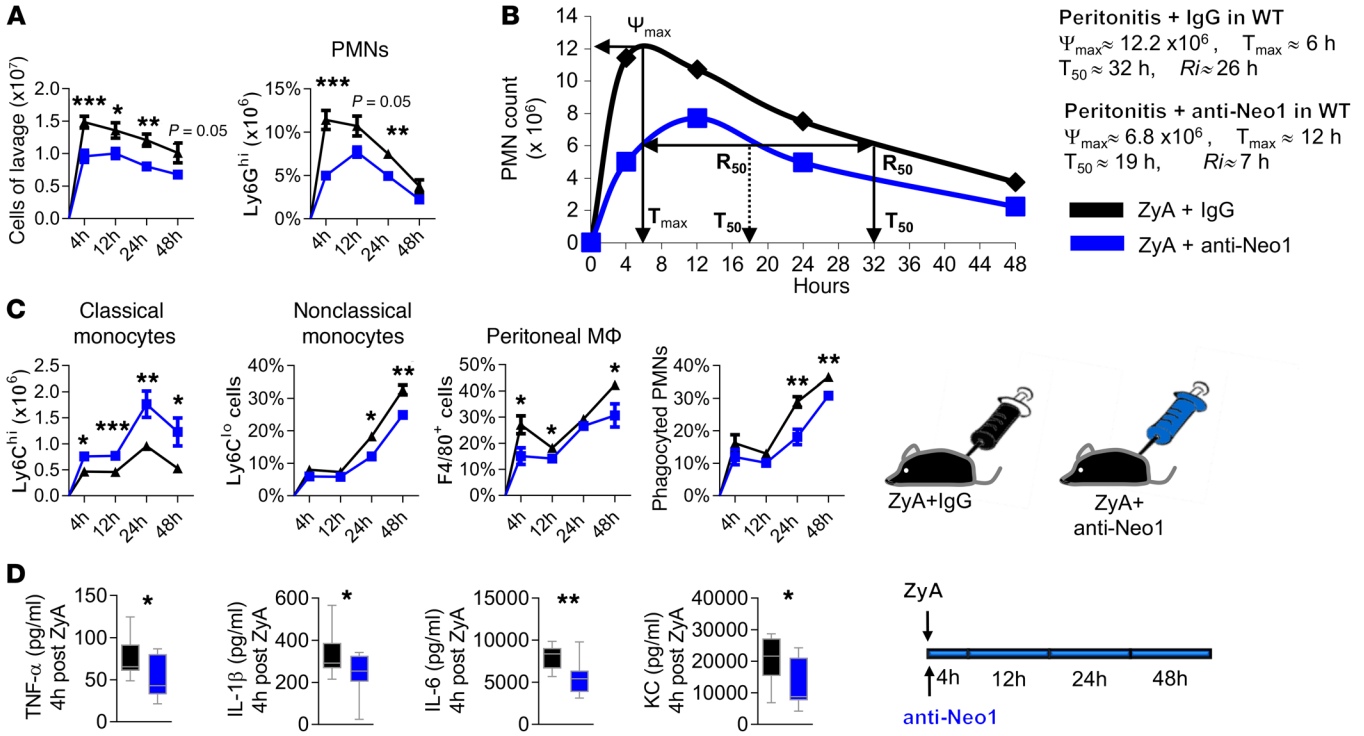

Figure 8. Exogenous inhibition of Neo1 attenuates inflammation and fosters resolution programs. WT mice were challenged with ZyA and subsequently injected with either IgG or a Neo1 inhibitory Ab, and lavages were collected at 4, 12, 24, and 48 hours. (**A**) The total leukocytes were enumerated by light microscopy, and the PMNs were determined by flow cytometry. (**B**) The resolution index was calculated as previously described (41). (**C**) Classical, nonclassical, peritoneal MΦ, and monocyte-derived MΦ efferocytosis were assessed by flow cytometry. (**D**) Proinflammatory cytokines TNF-α, IL-1β, IL-6, and KC 4 hours after ZyA injection. The therapeutic potential of Neo1 blockade was evaluated by application of anti-Neo1 Ab 4 hours after ZyA peritonitis induction at the peak of inflammation and peritoneal lavages were collected at 12, 24, and 48 hours. Results represent at least 2 independent experiments and are expressed as mean ± SEM (**A**, **C**) and median ± 95% CI (**D**) (n = 8–12 per group). Statistical analysis was done by unpaired Student's t test *P < 0.05; **P < 0.01; ***P < 0.001.

when anti-Neo1 Ab was given at the onset of inflammation. To further validate the proresolving attributes of the functional inhibition of Neo1, we examined the exudate IL-10 and TGF-β levels, which contribute to resolution and regenerative programs (18) (Figure 9C). Here, we found increased levels of both cytokines following anti-Neo1 Ab administration. To corroborate these results, we performed immunohistochemical characterization of PCNA, and found improved responses in tissue repair (Figure 9D). Finally, to clarify whether the loss of Neo1 with genetic deletion or with anti-Neo1 Ab treatment may blunt the initial inflammatory response, giving the false appearance of improved resolution, we first examined the biosynthesis of the lipid mediators specific to the resolution processes at a later time point (12 hours after ZyA injection), and found increased levels of specifically arachidonic acid–derived LXA_4 and DHA-derived PDX in Neo1$^{-/-}$ (Supplemental Figure 6, A–C). Then we exposed WT mice to ZyA peritonitis and this time the anti-Neo1 Ab was given in the resolution phase 6 hours after ZyA injection (e.g., regression of the neutrophil infiltration). The samples were collected 12 hours after ZyA injection. As expected, the collected data demonstrate that supplementation of anti-Neo1 6 hours after ZyA injection promotes the resolution/regeneration mechanism by decreasing the classical Ly6C^{hi} monocytes and increasing the nonclassical (M2) Ly6C^{lo} monocytes and macrophages that indicate a strong enhancement of macrophage clearance of apoptotic PMNs (Supplemental Figure 7). Studies have revealed Neo1 to be a specific receptor for 2 ligands, namely Netrin-1 and RGM-A (12, 13). We incubated peritoneal MΦ from WT and Neo1$^{-/-}$ mice with RGM-A or Netrin-1 to determine a possible influence on MΦ efferocytosis of fluorescent ZyA particles. Collected data revealed that RGM-A did not increase MΦ clearance in the Neo1$^{-/-}$ cells. When MΦ were stimulated with Netrin-1, efferocytosis was not significantly affected, suggesting that the actions of Neo1 are RGM-A dependent (Supplemental Figure 8).

These results indicate a critical role for the functional inhibition of Neo1 in controlling inflammation processes in the resolution and regeneration phases, and might demonstrate a possible therapeutic approach.

Plasma Neo1 is increased in critically ill pediatric patients with IAH or ACS and it is associated with clinical outcome. To translate our preclinical findings to humans, we investigated the association between Neo1 blood plasma levels and IAH grade, ACS, severity of illness, pediatric ICU (PICU) length of stay, and survival in a cohort of 59 critically ill pediatric patients partly suffering from abdominal compartment syndrome (ACS). In brief, we prospectively enrolled medical and surgical patients ranging in age from newborn to 17 years old with cardiac or oncological diseases, or after surgical interventions. In all enrolled subjects, intensive care monitoring was urgently indicated (i.e., admission

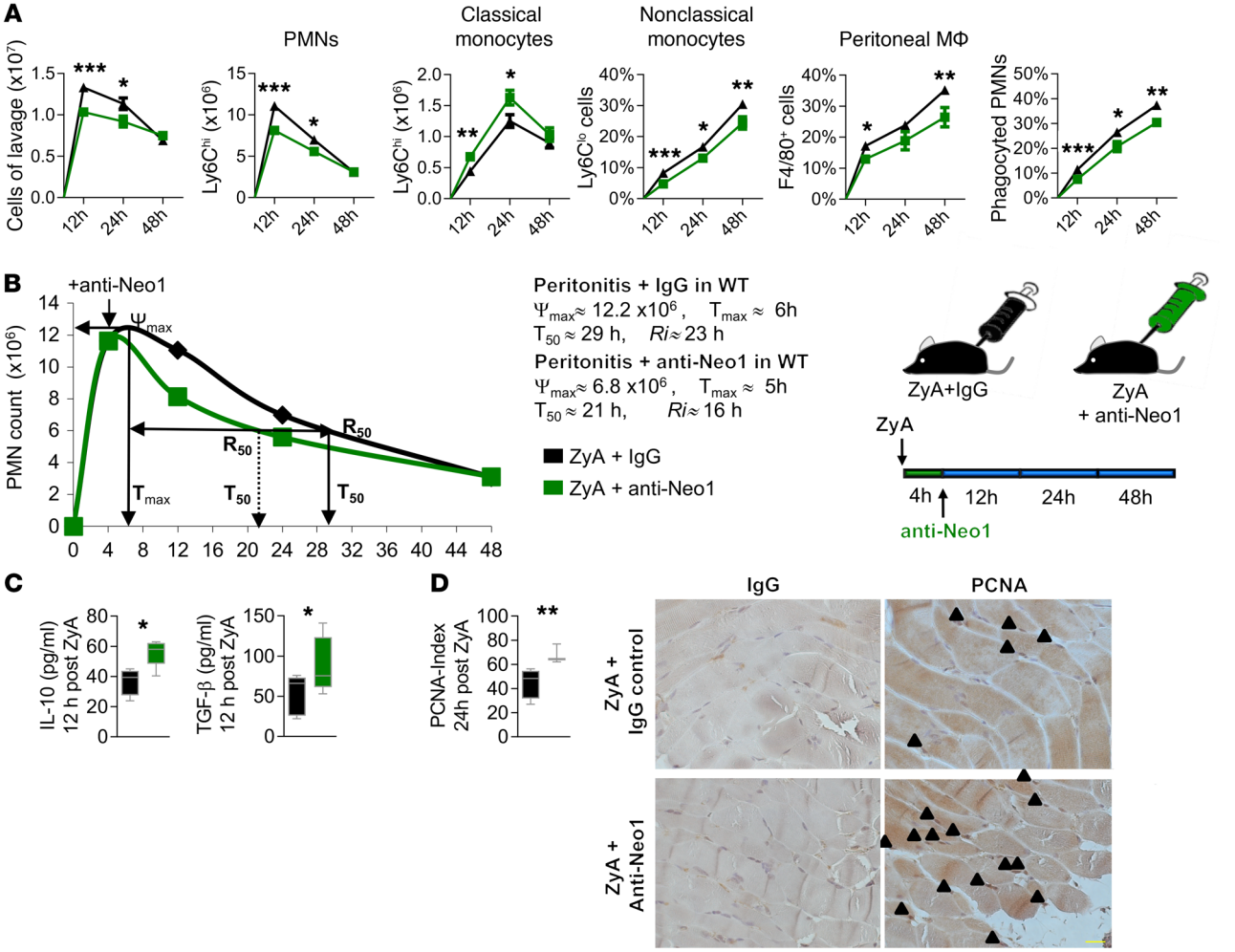

Figure 9. Exogenous therapeutic inhibition of Neo1 attenuates inflammation and fosters resolution programs. The therapeutic potential of Neo1 blockade was evaluated by application of anti-Neo1 Ab 4 hours after ZyA peritonitis induction at the peak of inflammation, and peritoneal lavages were collected at 12, 24, and 48 hours. (**A**) Total leukocyte cell numbers were enumerated and PMNs, classical and nonclassical monocytes, peritoneal MΦ, and monocyte-derived MΦ efferocytosis were measured by FACS. (**B**) Resolution index. (**C**) IL-10 and TGF-β levels 12 hours after ZyA injection. (**D**) PCNA immunohistochemistry images (n = 4/condition, magnification ×630, scale bar 200 μm) and the calculated PCNA index. Results represent at least 2 independent experiments and are expressed as mean ± SEM (**A**) and median ± 95% CI (**D**) (n = 8–12 per group). Statistical analysis was done by unpaired Student's t test, $^*P < 0.05$, $^{**}P < 0.01$, $^{***}P < 0.001$.

to PICU). Due to the different severities of the patients' illnesses, a selective division into 3 test groups was possible. The criteria were Pediatric Risk of Mortality III score (PRISM-III score), organ dysfunction, and intraabdominal pressure (IAP) level. Patient demographic and clinical data are shown in Figure 10, A and B, Table 1, Table 2, Supplemental Table 3, and Supplemental Table 4. The severity of illness was assessed by the PRISM-III score. The vital signs, other cardiorespiratory parameters, drug administration, IAP, and fluid balances were recorded continuously. With regard to ACS associated with substantial morbidity, such as renal failure and multiorgan dysfunction syndrome (MODS), and mortality in critically ill patients (33), our data revealed 1.8-fold higher Neo1 plasma concentrations in children with ACS versus those without ACS, and 1.7-fold higher plasma levels in children with ACS versus control ICU patients (Figure 10B). When comparing the Neo1 plasma levels with the severity of illness, we found that significantly increased levels of Neo1 in affected children correlated with PRISM-III score, IAH grade, and clinically established laboratory parameters such as serum C-reactive protein (CRP), lactate, creatinine, and bilirubin (Figure 10C). We also compared conventional laboratory inflammatory parameters with the above-mentioned organ and outcome parameters. Only CRP showed correlations comparable to those of Neo1 (related to Rho and P values). In contrast to Neo1, to our knowledge CRP has never shown any prognostic value with regard to the development of IAH or ACS. Only D-lactate was identified in the context of 2 animal studies as a biomarker for the development of ACS in the past (34, 35). In the pediatric literature, there is no study that would have identified a biomarker for the development of an AKS. Procalcitonin (PCT; n = 6) did show higher correlation coefficients (especially for creatinine, PICU length of stay, and PRISM-III scores); however, these results did not reach statistical significance, probably because PCT was only determined in 6 children on admission to our PICU (Supplemen-

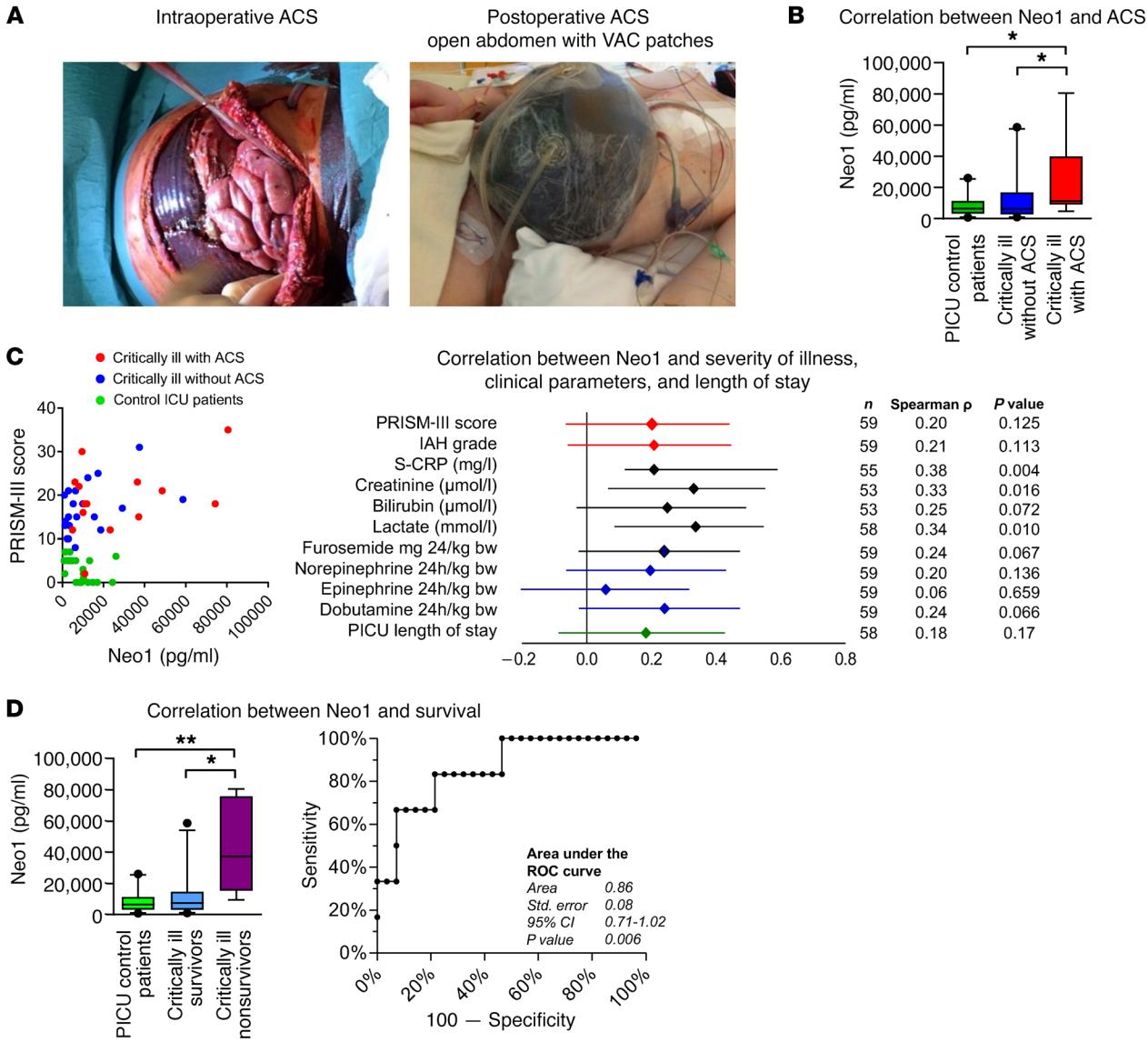

Figure 10. Neo1 in PICU patients with ACS. Plasma samples from 59 children with and without ACS were collected within 24 hours after admission to the PICU of Hannover Medical School (MHH). (**A**) Photos displaying the intraoperative situs during open abdomen therapy and the postoperative condition after the establishment of a belly-widening vacuum-assisted closure (VAC) wound dressing in children with fulminant ACS. (**B**) Value of Neo1 at the admission to the PICU was investigated by comparing the control group (Prism-III score <8), critically ill children without ACS (Prism-III score ≥8), and critically ill children meeting the 2013 WSACS definitions (38) for ACS. (**C**) Correlation between Neo1 and clinical parameters of all PICU patients enrolled. The Spearman's rank correlation coefficient Rho and the corresponding 95% CI interval are shown. (**D**) The predictive value of Neo1 at the admission to the PICU was investigated comparing PICU control patients (PRISM-III score <8), critically ill survivors (PRISM-III score ≥8), and critically ill nonsurvivors. An ROC curve was calculated comparing Neo1 in critically ill survivors with nonsurvivors. Patient characteristics for survivors and nonsurvivors. Results are displayed as median ± 95% CI. Statistical analysis was done by nonparametric Kruskal-Wallis test followed by Dunns post hoc test; correlation was tested using Spearman's rank correlation test, $*P < 0.05$, $**P < 0.01$.

tal Table 5). To clarify whether increased cell lysis might have caused an increase in membrane-bound Neo1 entering the plasma, we subsequently analyzed the serum concentrations of lactate dehydrogenase (LDH). All children enrolled into our study had a mild (non–critically ill [NCI] PICU controls) to marked increase (critically ill [CI] groups) in LDH serum concentration (normal reference values age-dependent, approximately <344 U/l). The difference in circulating LDH between controls and test groups was significant ($P = 0.03$). On the other hand, there was no significant difference between CI-ACS and CI+ACS ($P = 0.69$). Since plasma levels of Neo1 were significantly higher in the CI+ACS group than in the CI-ACS group, the results of LDH analysis thus indicate that the main source of Neo1 most likely does not arise from cell lysis (Supplemental Table 6). Moreover, the PICU length of stay was also correlated with increased levels of Neo1 (Figure 10C). Since mortality is one of the most reliable endpoints of clinical management in the ICU, we investigated whether plasma Neo1 could be a mortality predictor in critically ill children. We found Neo1 to be 5.0-fold higher in nonsurvivors compared with survivors and 5.7-fold higher in nonsurvivors

Table 1. Correlation between Neo1 and ACS in PICU patients with ACS

	Number of patients	Male sex, *n* (%)	Prism-III score, median (min-max)	Age in months, median (min-max)	Days of PICU stay, median (min-max)	Primary reason for PICU admission				
						Postsurgery	Hemic-oncological	Cardiology	Sepsis	Postneurosurgery
PICU control patients	25	9 (36)	5.0 (0–7)	15.0 (0–199)	1.0 (0–20)	7	3	6	0	9
Critically ill without ACS	20	10 (50)	16.0 (8–31)	31.5 (0–199)	4.0 (1–18)	6	0	13	0	1
Critically ill with ACS	14	7 (50)	18.0 (2–35)	28.0 (0–190)	19.5 (1–332)	8	1	4	1	0

Overview of PICU patient characteristics within the control group (Prism-III score <8), critically ill children without ACS (Prism-III score ≥8), and critically ill children meeting the 2013 WSACS definitions for ACS.

compared with ICU controls. Receiver operating curve (ROC) analysis comparing survivors with nonsurvivors demonstrated a strong specificity (92.86%, sensitivity 66.67%) for Neo1 plasma levels greater than 36.777 pg/ml, indicating that Neo1 can be a valid predictor of mortality (Figure 10D).

Discussion

Results from the present report reveal that the neuronal guidance protein Neo1 contributed not only to the onset of an inflammatory response but also to local inflammation resolution mechanisms and tissue regeneration processes. In this report, we demonstrated that genetic deletion or functional inhibition of Neo1 led to a reduction in neutrophil recruitment at the injury sites and abbreviation of neutrophil lifespan by increasing apoptosis and ultimately inducing MΦ clearance. The biosynthesis of endogenous SPMs and their pathway markers was enhanced in *Neo1*$^{-/-}$ mice, and the regeneration of tissue injury was improved. Treatment with an anti-Neo1 Ab demonstrated reduced inflammatory status, indicating acceleration in resolution and promotion of tissue repair. In a cohort that included critically ill PICU patients, we found associations between plasma Neo1 and IAH grade, ACS, PRISM-III score, PICU length of stay, and survival. Together these data point toward a crucial role of Neo1 in the initiation and resolution of inflammatory and resolving/regenerative processes.

Inflammation driven by tissue injury or infection is characterized as modular in its temporal sequence of events, and this is critical for survival. An acute inflammatory response is divided into distinct phases: the initiation phase and the resolution/regeneration phase. The initiation phase (proinflammatory early state) comprises the migration of key inflammatory cells to the site of inflammation, guided by chemical messengers such as cytokines, chemokines, and lipid mediators (23, 36). The resolution of the inflammatory response is a precisely controlled active process governed by local SPMs that mediate the clearance and killing, efferocytosis, and phagocytosis of apoptotic PMNs to restore tissue homeostasis after injury and phlogistic processes (5).

A group of guidance proteins was originally recognized for its role in the developing nervous system. Considering the similarities between neuronal cell guidance and leukocyte trafficking, recent studies have pointed to additional roles for NGPs in modulating the inflammatory response outside the CNS (6–8, 10, 37, 38). A crucial target receptor in mediating NGP function in the CNS is the Neo1 receptor. Its function is best described in the nervous system where it guides cell and axon migration during embryonic development (14). Neo1 provides chemoattractive and chemorepulsive attributes, depending on its ligand binding (12). More recently, Lee et al. demonstrated a crucial role for Neo1 in the control of junctional stability during epithelial morphogenesis (39). Neo1 has been studied at the onset of inflammation (9, 15, 38) in peripheral organs; however, its role during the resolution and regeneration phases, particularly the understanding of pathways that can promote or mitigate the resolution of inflammation, remains unclear. Considering that failed clearance of apoptotic cells modifies immune tolerance and promotes nonresolving inflammation (17) (i.e., sepsis), we investigated the role of Neo1 in the apoptosis of neutrophils. The inhibition of Neo1 led to an increase of the find-me signals CX_3CL1 and CX_3CR1, the decoy receptor IL-1R2, and the eat-me receptor TIM4 in human apoptotic PMNs or MΦ, and the efferocytosis of apoptotic PMNs was substantially enhanced. In murine peritonitis, Neo1$^{-/-}$ deficiency displayed enhanced neutrophil apoptosis. This was accompanied by decreased recruitment of classical Ly6C^{hi} cells and an increased population of alternatively activated Ly6C^{lo} and conclusively

Table 2. Correlation between Neo1 and survival in PICU patients with ACS

	Critically ill survivors	Critically ill nonsurvivors
Number of patients	28	6
Male sex, *n* (%)	13 (36)	4 (60)
Prism-III score, median (min–max)	16.5 (2–23)	27.5 (15–35)
Age in months, median (min–max)	29.5 (0–199)	35.5 (0–190)
Days of PICU stay, median (min–max)	7.5 (1–332)	8.5 (1–30)
Primary reason for admission to PICU		
Postsurgery	11	3
Hemic-oncological	0	1
Cardiology	15	2
Sepsis	1	0
Postneurosurgery	1	0

Overview of PICU patient characteristics for survivors and nonsurvivors.

enhanced efferocytosis of apoptotic PMNs. When investigating the role of Neo1 more precisely, we found that in bone marrow and peritoneal monocytes there was a strong reduction of the migratory classical Ly6C^{hi} cells in the peritoneal cavity of Neo1$^{-/-}$ mice. Neo1 expression was restricted to the peritoneal inflammatory Ly6C^{hi} cells, suggesting that the lack of Neo1 induced a phenotypic switch toward the antiinflammatory and proresolving M2 type. To show in more detail that Neo1 has a direct influence on classical and nonclassical monocytes and efferocytosis, we carried out additional experiments. We exposed bone marrow chimeric mice to ZyA peritonitis and analyzed the leukocytes and clearance at 4 hours and 12 hours after ZyA injection. As expected, bone marrow chimeric animals with hematopoietic Neo1 repression demonstrated a reduction in classical Ly6C^{hi} cells, an increase in nonclassical Ly6C^{lo} monocytes, and finally a strong enhancement of the efferocytic capacity at both time points. As demonstrated before, Ly6C, which is known to be mainly expressed on the migrating proinflammatory monocytes, was markedly decreased in peritoneal Neo1$^{-/-}$ monocytes compared with littermate controls. This influence was also noted in the bone marrow chimeric animals with hematopoietic Neo repression. Ly6C MFI was markedly decreased in Ly6C^{hi} cells in bone marrow chimeric animals with hematopoietic Neo repression, implying that Neo1 may impact the proinflammatory Ly6C^{hi} monocytes.

At the signaling level, we were able to demonstrate the activation of the PI3K/AKT pathway and the suppression of the TGF-β pathway in Neo1$^{-/-}$ monocytes. Specifically, the activation of the PI3K/AKT pathway has been reported to be a crucial step toward the proresolving M2 phenotype (26).

Since the resolution of inflammation is induced to a large extent by SPMs, the generation of several of these endogenous classes of SPMs and their pathway markers (i.e., LXA_4, Mar1, and PDX) were markedly enhanced in Neo1$^{-/-}$ exudates. Likewise, the metabolites 13,14-diHETE and 19,20-diHDPA, which belong to a different class of antiinflammatory and proresolving lipids and are produced by cytochrome P450, were strongly increased in Neo1-deficient mice compared with their littermate controls. Also, the resolution interval was shortened from 27 hours to 9 hours. The decreased levels of IL-6, KC, MIP2, and MCP-1 within the Neo1$^{-/-}$ peritonitis lavages collected in the resolution phase 12 hours after ZyA injection underlined the effect of Neo1 on the resolution phase. When determining the therapeutic efficacy of Neo1 in resolving processes, we found that both the prophylactic and the therapeutic functional inhibition of Neo1 activated inflammation resolution programs and promoted tissue regeneration as demonstrated by reduced PMN recruitment, decreased classical Ly6C^{hi} monocytes, and increased nonclassical Ly6C^{lo} monocytes and MΦ, which led to the strong enhancement of MΦ clearance of apoptotic PMNs. The exudate IL-10 and TGF-β levels that contributed to the resolution and regenerative programs (18) were strongly enhanced. The improved tissue repair responses analyzed by PCNA corroborate the critical role for Neo1 in the resolution and regenerative processes. Finally, to clarify the question of whether the loss of Neo1 with genetic deletion or with anti-Neo1 Ab treatment may blunt the initial inflammatory response, giving the false appearance of improved resolution, we injected the anti-Neo1 Ab in the resolution phase 6 hours after ZyA injection, and found anti-Neo1 treatment to have a strong impact on key characteristics of resolution. It is evident that critically ill patients might display severe comorbidities that are a major threat to global health. In fact, clinical trials may be the most effective way to investigate the usefulness of novel predictive indications. Therefore, in a cohort of critically ill PICU patients suffering in part from ACS, we found a strong correlation between Neo1 plasma levels and ACS, IAH grade, PRISM-III disease severity score, ICU length of stay, and survival.

In conclusion, our study reveals a key role for Neo1 in controlling inflammation resolution and regeneration programs. Our findings demonstrate that deficiency of Neo1 directly promotes antiinflammatory, proresolving effects (i.e., shortening of resolution phase, activating SPM generation, reducing PMN influx, activating PMN apoptosis, and increasing MΦ phagocytosis of apoptotic PMNs). Moreover, our data revealed that Neo1 correlates with ACS, PRISM-III score, ICU length of stay, and survival in critically ill children, and might therefore evolve as a new clinical marker and therapeutic target in inflammatory conditions.

Methods

Animals. This project was approved by the institutional review board and the Regierungspräsidium Tübingen. WT (C57BL/6N), *Neo1*$^{-/-}$ (C57BL/6N-Neo1$^{Gt(KST265)Byg}$), and littermate control mice (C57BL/6N) were bred and genotyped as previously described (8). At 8 to 10 weeks old, mice of either sex were assigned to the respective study time points and/or experimental interventions at random.

Murine peritonitis. All animal protocols were performed in accordance with the regulations of the Regierungspräsidium Tübingen and the local ethics committee. All trials took into account Directive 2010/63/EU adopted by the European Parliament and Council. The mice were intraperitoneally injected with 1 ml zymosan A (ZyA; 1 mg/ml; Sigma-Aldrich, catalog Z4250) and subsequently intravenously with either IgG control (Santa Cruz Biotechnology, catalog sc-2028) or 2 μg Neo1 blocking antibody (R&D Systems, catalog AF-1079) in a total volume of 150 μl. Peritoneal fluids and tissues were obtained at 4, 12, 24, and 48 hours and prepared as previously described (37). The collected exudates were washed, suspended in PBS (Millipore-Sigma), and counted.

Differential leukocyte counts, FACS analysis, and cytokines. Exudate cells from the murine peritonitis models were prepared to determine their cellular composition. The cells were blocked with mouse anti-CD16/CD32 (Biolegend, catalog 101320) antibodies for 10 minutes at room temperature and then stained with anti-mouse APC-Ly6G (BioLegend, catalog 127614), e450-F4/80 (eBioscience, catalog 48-4801-82), and FITC-Ly6C (BioLegend, catalog 128006) antibodies for 30 minutes at 4°C. To analyze the MΦ phagocytosis of apoptotic PMNs in vivo, the cells were permeabilized using a fixation and permeabilization kit (BD Biosciences, catalog 554714) prior to staining with PerCP-Cy5.5–conjugated anti-Ly6G (BioLegend, catalog 127616) for 30 minutes at 4°C. The cells were acquired on a FACSCanto II (BD Biosciences) and analyzed with FlowJo (Tree-Star). Cytokines were measured in the murine peritoneal exudates using standard ELISA (R&D Systems).

Lipid mediator lipidomics. LC-MS/MS analysis was carried out as previously described with some modifications (40, 41). Peritoneal lavage samples were thawed, and internal standards were added and subsequently extracted twice using methanol. The combined organ-

ic extracts were cleaned up using solid-phase extraction according to published protocols (41). LC-MS/MS analysis was carried out using a 6500 QTrap LC-MS/MS system as previously described (40). For a detailed description of the analytical procedure please refer to the Supplemental Material.

Antibody array for protein expression. Peritoneal monocytes/macrophages from WT and $Neo^{-/-}$ mice were used following 12 hours of ZyA-induced peritonitis. Protein and phosphorylation (TGF-β Phospho Antibody Array, Full Moon BioSystems, catalog PTG176) profiling of peritoneal monocytes (pooled lavages from 4 mice/condition) was carried out according to the manufacturer's instructions. The images were acquired by the manufacturer. For each antibody, the average signal intensity of 6 replicates was normalized to the median signal of all antibodies on the array. The presented fold change represents the ratio of the normalized signal from $Neo1^{-/-}$ mice compared with WT littermate controls. GAPDH and beta-actin were used as housekeeping proteins. Data analysis was performed with IPA software (Qiagen). Pathways were substantiated and updated with recent literature, the KEGG database (HSA 04350, HAS 04151; https://www.genome.jp/kegg/), and the Reactome database (R-HSA-198203, R-HSA-2173789; https://reactome.org/). Data were deposited in the NCBI's Gene Expression Omnibus database (GEO GSE117137) (42).

Human PMN apoptosis and MΦ efferocytosis. PMNs and human peripheral blood monocytes were isolated from healthy volunteers or human leukapheresis collars from the Blood Bank of Eberhard Karls University of Tübingen by gradient centrifugation using Histopaque-1077 (MilliporeSigma). Monocytes were cultured in RPMI 1640 medium (MilliporeSigma) with 10 ng/ml human recombinant GM-CSF (Milteny Biotec, catalog 130-093-866) at 37°C in 5% CO_2 for 7 days. Human PMNs were labeled with carboxyfluorescein diacetate (10 μM, 30 minutes at 37°C; Molecular Probes) and allowed to undergo apoptosis in serum-free RPMI 1640 medium (Gibco) for 16 to 18 hours. GM-CSF–differentiated MΦ (0.1×10^6 cells/well) were then incubated with human Neo1 Ab (R&D Systems, catalog AF1079) or IgG control (Santa Cruz Biotechnology, catalog sc-2028) for 15 minutes. Apoptotic PMNs were added in a 1:3 ratio (MΦ/PMNs) and incubated at 37°C for 60 minutes to allow phagocytosis. In a separate experiment, GM-CSF–differentiated MΦ were incubated with Neo1 Ab (R&D Systems, catalog AF1079) or IgG control (Santa Cruz Biotechnology, catalog sc-2028) for 15 minutes at 37°C and then incubated with fluorescently labeled (BacLight; Thermo Fisher Scientific, catalog B35000) *E. coli* at a 1:50 ratio for 60 minutes. Efferocytosis was determined using a fluorescent plate reader (Tecan).

To evaluate PMN apoptosis, PMNs were incubated in RPMI 1640 (Gibco) plus 10% FCS in the presence or absence of LPS (MilliporeSigma, catalog LA4391) and/or Neo1-antibody (R&D Systems, catalog AF1079) for 20 hours at 37°C in 5% CO_2. Apoptosis was measured by FACS analysis using an Annexin V PE apoptosis detection kit with 7-AAD (BioLegend, catalog 640934) according to the manufacturer's instructions, and transcriptional analysis was performed.

Transcriptional analysis of human MΦ and PMNs. Human GM-CSF–differentiated MΦ were incubated in RPMI 1640 (Gibco) in the presence or absence of IL-1β (Promokine, catalog C-61120) and/or anti-Neo1 antibody (R&D Systems, catalog AF1079) for 4 hours prior to transcriptional analysis. Human *18S* expression as a housekeeping gene was evaluated with the sense primer 5′-GTAACCCGTTGAACCCCATT-3′ and antisense primer 5′-CCATCCAATCGGTAGTAGCG-3′. The following primers were used: *Cx3cl1:* 5′-CGGTGTGACGAAATGCAACA-3′, 5′-CTCCAAGATGATTGCGCGTTT-3′; *Il1r2:* 5′-GTGAGCAACAAGGCC A-3′, 5′-TACCAACACGTACAAGCGCA-3′; *Cx3cr1:* 5′-GAGGCGTTTAAGTTGGCAGA-3′, 5′-ATGGTGAAGGCCCCACT-3′; *Tim4:* 5′-ACAGGACAGATGGATGGAATACCC-3′, 5′-AGCCTTGTGTGTTTCTGCG-3′; *Gpr32:* 5′-GGGCCTGCAAACTCTACA-3′, 5′-GGAGGCAGTTACTGGCAA-3′; *Alx/Fpr:* 5′-TGTTCTGCGGATCCTCCCATT-3′, 5′-CTCCCATGGCCATGGAGACA-3′.

Cytology, immunofluorescence, and immunohistochemistry staining. GM-CSF–differentiated human MΦ were stimulated for 4 hours with IL-1β (Promokine, catalog C-61120) prior to labeling with rabbit anti-Neo1 (Santa Cruz Biotechnology, catalog sc-15337) and rhodamine phalloidin (Invitrogen, catalog R415). An IgG isotype control antibody (Santa Cruz Biotechnology, catalog sc-2027) was used as a negative control. Alexa Fluor 488–conjugated goat anti-rabbit (Life Technologies, catalog A27034) was used as the secondary antibody. DAPI (4′,6-diamidino-2-phenylindole; Invitrogen, catalog P36931) was employed for nuclear counterstaining. For immunofluorescence analysis of human MΦ efferocytosis of fluorescently labeled PMNs, MΦ were stained with mouse-anti-CD14 (Santa Cruz Biotechnology, catalog sc-58951) and A594 goat-anti-mouse secondary antibody (Thermo Fisher Scientific, catalog A-11005). DAPI (Invitrogen, catalog P36931) was employed for nuclear counterstaining. Immunofluorescence images were acquired using a confocal microscope (LSM 510 Meta fluorescence microscope, Carl Zeiss) and ZEN software (Carl Zeiss). To perform immunohistochemical staining for PCNA, paraffin-embedded peritoneal tissues were stained with an anti-PCNA antibody (Santa Cruz Biotechnology, catalog sc-56) using a Vectastain ABC Kit (Vector Labs, catalog PK-4004) and DAB peroxidase substrate (Sigma-Aldrich, catalog E109) according to the manufacturers' instructions. As the secondary antibody, a biotin-conjugated horse-anti-mouse antibody (Vector Labs, catalog BA-2000) was used. The sections were then counterstained with hematoxylin. Light microscopy images were acquired with a DM IRM microscope (Leica) equipped with an AxioCam MRc (Carl Zeiss) using AxioVision software (Carl Zeiss).

Pediatric ICU patient samples with and without ACS. A total of 59 plasma samples were taken from patients from the PICU of Hannover Medical School (MHH) within 24 hours after admission. The 2013 WSACS definitions (43) (with respect to IAP and ACS; www.wsacs.org) were used to define the ACS. Severity of illness in the ICU children was measured using PRISM-III scoring (44).

Vital and cardiorespiratory parameters (including ventilation parameters), drug administration, intraabdominal pressure (measured via gastric Spiegelberg monitoring system) (45), and fluid balances were recorded continuously via the digital patient data management system (mlife, mediside). A Neo1 ELISA (Cusabio, catalog CSB-EL015712HU) was performed according to manufacturer's instructions. For a detailed description of the criteria for patient selection and monitoring please refer to the Supplemental Material.

Statistics. Statistical analysis of murine and in vitro data was performed using ANOVA with Bonferroni's multiple comparisons test. An unpaired 2-tailed Student's *t* test was used to compare 2 independent groups. Experimental data are reported as mean ± SEM. Statistical analyses of data from PICU patients were performed using the nonparametric Kruskal-Wallis test followed by Dunn's multiple compari-

sons test. Data are reported as median ± 95% CI. Correlation of clinical data was tested using Spearman's rank correlation test. For all tests, a *P* value less than 0.05 was considered statistically significant. Analyses were performed using GraphPad Prism5 (GraphPad Software) and JMP 13 (SAS).

Study approval. Critically ill children newborn to age 17 years were enrolled between January and August 2015 after informed written consent was obtained from the parents or guardians of each child. The study was approved by the local ethics committee (Ethikkommission der MHH, Hannover, Germany) of Hannover Medical School (MHH 6677) and internationally registered (WHO-ICTRP DRKS00006556). Animal experiments were approved by the institutional review board and the Regierungspräsidium Tübingen (Tübingen, Germany).

Author contributions

MS, AK, CG, and UK performed the experiments, and collected and analyzed the data. TK and GH performed the clinical experiments in patients. HSJ and MG performed the targeted lipidomic and lipid mediator analysis studies. All authors contributed to manuscript preparation and figure preparation. VM carried out overall experimental design, conceived of the overall research, and wrote the manuscript.

Acknowledgments

We thank Alice Mager, Hannes Frohnmeyer, and Marieke Heijink for their technical support. This work was supported by grants from the Interdisziplinäres Zentrum für Klinische Forschung (IZKF; 2110-0-0) and the Deutsche Forschungsgemeinschaft (DFG-MI 1506/4-1 and DFG-MI 1506/5-1) to VM; by IZKF fortüne grants to MS (2299-0-0) and AK (2377-0-0); and by an intramural grant from the Hannover Medical School (Junge Akademie/MHH Young Academy grant 9790012) to TK.

Address correspondence to: Valbona Mirakaj, Department of Anesthesiology and Intensive Care Medicine, Molecular Intensive Care Medicine, Eberhard-Karls University, Hoppe-Seyler-Straße 3, 72076 Tübingen, Germany. Phone: 49.7071.29.86344; Email: valbona.mirakaj@uni-tuebingen.de.

1. Ferreira FL, Bota DP, Bross A, Mélot C, Vincent JL. Serial evaluation of the SOFA score to predict outcome in critically ill patients. *JAMA*. 2001;286(14):1754–1758.
2. Nathan C, Ding A. Nonresolving inflammation. *Cell*. 2010;140(6):871–882.
3. Kotas ME, Medzhitov R. Homeostasis, inflammation, and disease susceptibility. *Cell*. 2015;160(5):816–827.
4. Baggiolini M. Chemokines and leukocyte traffic. *Nature*. 1998;392(6676):565–568.
5. Serhan CN. Pro-resolving lipid mediators are leads for resolution physiology. *Nature*. 2014;510(7503):92–101.
6. Rosenberger P, et al. Hypoxia-inducible factor-dependent induction of netrin-1 dampens inflammation caused by hypoxia. *Nat Immunol*. 2009;10(2):195–202.
7. Mirakaj V, et al. Netrin-1 dampens pulmonary inflammation during acute lung injury. *Am J Respir Crit Care Med*. 2010;181(8):815–824.
8. Mirakaj V, et al. Repulsive guidance molecule-A (RGM-A) inhibits leukocyte migration and mitigates inflammation. *Proc Natl Acad Sci U S A*. 2011;108(16):6555–6560.
9. Mirakaj V, Jennewein C, König K, Granja T, Rosenberger P. The guidance receptor neogenin promotes pulmonary inflammation during lung injury. *FASEB J*. 2012;26(4):1549–1558.
10. van Gils JM, et al. The neuroimmune guidance cue netrin-1 promotes atherosclerosis by inhibiting the emigration of macrophages from plaques. *Nat Immunol*. 2012;13(2):136–143.
11. Mirakaj V, Rosenberger P. Immunomodulatory functions of neuronal guidance proteins. *Trends Immunol*. 2017;38(6):444–456.
12. Rajagopalan S, et al. Neogenin mediates the action of repulsive guidance molecule. *Nat Cell Biol*. 2004;6(8):756–762.
13. Wilson NH, Key B. Neogenin: one receptor, many functions. *Int J Biochem Cell Biol*. 2007;39(5):874–878.
14. Vielmetter J, et al. Molecular characterization of human neogenin, a DCC-related protein, and the mapping of its gene (NEO1) to chromosomal position 15q22.3-q23. *Genomics*. 1997;41(3):414–421.
15. König K, Gatidou D, Granja T, Meier J, Rosenberger P, Mirakaj V. The axonal guidance receptor neogenin promotes acute inflammation. *PLoS ONE*. 2012;7(3):e32145.
16. Schlegel M, et al. Inhibition of neogenin dampens hepatic ischemia-reperfusion injury. *Crit Care Med*. 2014;42(9):e610–e619.
17. Ravichandran KS. Beginnings of a good apoptotic meal: the find-me and eat-me signaling pathways. *Immunity*. 2011;35(4):445–455.
18. Serhan CN, Savill J. Resolution of inflammation: the beginning programs the end. *Nat Immunol*. 2005;6(12):1191–1197.
19. Filep JG. Resolution of inflammation: leukocytes and molecular pathways as potential therapeutic targets. *Front Immunol*. 2013;4:256.
20. Bourke E, Cassetti A, Villa A, Fadlon E, Colotta F, Mantovani A. IL-1 beta scavenging by the type II IL-1 decoy receptor in human neutrophils. *J Immunol*. 2003;170(12):5999–6005.
21. Ortega-Gómez A, Perretti M, Soehnlein O. Resolution of inflammation: an integrated view. *EMBO Mol Med*. 2013;5(5):661–674.
22. Truman LA, et al. CX3CL1/fractalkine is released from apoptotic lymphocytes to stimulate macrophage chemotaxis. *Blood*. 2008;112(13):5026–5036.
23. Buckley CD, Gilroy DW, Serhan CN. Proresolving lipid mediators and mechanisms in the resolution of acute inflammation. *Immunity*. 2014;40(3):315–327.
24. Jakubzick CV, Randolph GJ, Henson PM. Monocyte differentiation and antigen-presenting functions. *Nat Rev Immunol*. 2017;17(6):349–362.
25. Quintar AA, Hedrick CC, Ley K. Monocyte phenotypes: when local education counts. *J Exp Med*. 2015;212(4):432.
26. Manning BD, Toker A. AKT/PKB signaling: navigating the network. *Cell*. 2017;169(3):381–405.
27. Covarrubias AJ, et al. Akt-mTORC1 signaling regulates Acly to integrate metabolic input to control of macrophage activation. *Elife*. 2016;5:e11612.
28. Chen W, Ten Dijke P. Immunoregulation by members of the TGFβ superfamily. *Nat Rev Immunol*. 2016;16(12):723–740.
29. Zhang Y, et al. Tissue regeneration. Inhibition of the prostaglandin-degrading enzyme 15-PGDH potentiates tissue regeneration. *Science*. 2015;348(6240):aaa2340.
30. Dalli J, Serhan C. Macrophage proresolving mediators-the when and where. *Microbiol Spectr*. https:/doi.org/10.1128/microbiolspec.MCHD-0001-2014.
31. Levy BD, Clish CB, Schmidt B, Gronert K, Serhan CN. Lipid mediator class switching during acute inflammation: signals in resolution. *Nat Immunol*. 2001;2(7):612–619.
32. van der Wal JB, Jeekel J. Biology of the peritoneum in normal homeostasis and after surgical trauma. *Colorectal Dis*. 2007;9 Suppl 2:9–13.
33. Kirkpatrick AW, et al. Update from the Abdominal Compartment Society (WSACS) on intra-abdominal hypertension and abdominal compartment syndrome: past, present, and future beyond Banff 2017. *Anaesthesiol Intensive Ther*. 2017;49(2):83–87.
34. Nielsen C, Kirkegård J, Erlandsen EJ, Lindholt JS, Mortensen FV. D-lactate is a valid biomarker of intestinal ischemia induced by abdominal compartment syndrome. *J Surg Res*. 2015;194(2):400–404.
35. Duzgun AP, et al. The relationship between intestinal hypoperfusion and serum d-lactate levels during experimental intra-abdominal hypertension. *Dig Dis Sci*. 2006;51(12):2400–2403.
36. Eming SA, Wynn TA, Martin P. Inflammation and metabolism in tissue repair and regeneration. *Science*. 2017;356(6342):1026–1030.
37. Mirakaj V, Dalli J, Granja T, Rosenberger P, Serhan CN. Vagus nerve controls resolution and pro-resolving mediators of inflammation. *J Exp Med*. 2014;211(6):1037–1048.
38. Schlegel M, et al. The neuroimmune guidance cue netrin-1 controls resolution programs

and promotes liver regeneration. *Hepatology*. 2016;63(5):1689–1705.
39. Lee NK, et al. Neogenin recruitment of the WAVE regulatory complex maintains adherens junction stability and tension. *Nat Commun*. 2016;7:11082.
40. Heemskerk MM, et al. Prolonged niacin treatment leads to increased adipose tissue PUFA synthesis and anti-inflammatory lipid and oxylipin plasma profile. *J Lipid Res*. 2014;55(12):2532–2540.
41. Giera M, et al. Lipid and lipid mediator profiling of human synovial fluid in rheumatoid arthritis patients by means of LC-MS/MS. *Biochim Biophys Acta*. 2012;1821(11):1415–1424.
42. Edgar R, Domrachev M, Lash AE. Gene Expression Omnibus: NCBI gene expression and hybridization array data repository. *Nucleic Acids Res*. 2002;30(1):207–210.
43. Kirkpatrick AW, et al. Intra-abdominal hypertension and the abdominal compartment syndrome: updated consensus definitions and clinical practice guidelines from the World Society of the Abdominal Compartment Syndrome. *Intensive Care Med*. 2013;39(7):1190–1206.
44. Pollack MM, et al. The Pediatric Risk of Mortality Score: update 2015. *Pediatr Crit Care Med*. 2016;17(1):2–9.
45. Malbrain ML, De laet I, Viaene D, Schoonheydt K, Dits H. In vitro validation of a novel method for continuous intra-abdominal pressure monitoring. *Intensive Care Med*. 2008;34(4):740–745.